Mechanics Research Communications 127 (2023) 104023

Contents lists available at ScienceDirect

Mechanics Research Communications

journal homepage: www.elsevier.com/locate/mechrescom

Geometric modelling of polycrystalline materials: Laguerre tessellations and periodic semi-discrete optimal transport

D.P. Bourne [a,*], M. Pearce [a], S.M. Roper [b]

[a] Maxwell Institute for Mathematical Sciences and Department of Mathematics, Heriot-Watt University, Edinburgh, UK
[b] School of Mathematics and Statistics, University of Glasgow, Glasgow, UK

ARTICLE INFO

Keywords:
Laguerre diagrams
Power diagrams
Polycrystalline materials
Grains
Semi-discrete optimal transport theory

ABSTRACT

In this paper we describe a fast algorithm for generating periodic RVEs of polycrystalline materials. In particular, we use the damped Newton method from semi-discrete optimal transport theory to generate 3D periodic Laguerre tessellations (or power diagrams) with cells of given volumes. Complex, polydisperse RVEs with up to 100,000 grains of prescribed volumes can be created in a few minutes on a standard laptop. The damped Newton method relies on the Hessian of the objective function, which we derive by extending recent results in semi-discrete optimal transport theory to the periodic setting.

1. Introduction

There is a large literature on geometric modelling of polycrystalline metals and foams using Laguerre tessellations and weighted Voronoi diagrams; see for example the following recent papers and their references: [1–7]. Applications include generating representative volume elements (RVEs) for computational homogenisation [8,9], fitting Laguerre tessellations to imaging data of polycrystalline microstructures [10,11], and modelling grain growth [12].

This paper builds on the research programme initiated in [2], where recent results from optimal transport theory [13] were exploited to develop fast algorithms for generating Laguerre tessellations with grains of given volumes. These ideas were developed further by [3] (see below) and applied by [8] to study biopolymer aerogels. In this paper we improve the speed of the algorithm from [2].

This paper also extends some theoretical results in semi-discrete optimal transport theory from [14,15] to the periodic quadratic cost function (see Theorem 2.5). This extension to periodic domains was driven by applications, not only by the application to microstructure modelling (where the RVEs should be periodic to avoid artificial boundary effects in computational homogenisation), but also by a recent application in weather modelling [16].

Outline of the paper. Section 2 includes the mathematical theory of periodic semi-discrete optimal transport. In particular, in Section 2.2 we recall that periodic Laguerre tessellations with cells of given volumes can be generated by maximising the concave function $\mathcal{K}^\Lambda$, defined in Eq. (2.2). In [2] $\mathcal{K}^\Lambda$ is maximised using a 1st-order method (the 2nd-order damped Newton method of [14] was also proposed but not implemented). Faster optimisation methods for maximising $\mathcal{K}^\Lambda$ were implemented in [3], including the Barzilai–Borwein method and a modified Newton method.

In this paper we implement the damped Newton method of [14], where the concave function $\mathcal{K}^\Lambda$ is maximised by applying Newton's method with a bespoke backtracking scheme to the nonlinear equation $\nabla\mathcal{K}^\Lambda = 0$. This requires an expression for the Hessian of $\mathcal{K}^\Lambda$, which does not appear in the literature as far as we are aware ([14] does not include it since the periodic quadratic transport cost is not differentiable). We derive it in Theorem 2.5.

In Section 3 we state the damped Newton method of [14] before applying it to microstructure modelling in Section 4. In particular, we combine the damped Newton method with [2, Algorithm 2] to develop a fast algorithm for generating RVEs with grains of given volumes. In Example 4.1 we generate a polydisperse RVE with 10,000 grains of given volumes in less than a minute on a standard laptop, and in Section 5 we generate RVEs with 100,000 grains in a matter of minutes. In Section 5 we also study the number of Newton iterations and backtracking steps for the damped Newton method.

Summary of main contributions.

- Theorem 2.5: We prove that the Kantorovich function $\mathcal{K}^\Lambda$ is twice differentiable (under suitable assumptions) and compute its Hessian. This extension of some results from [14,15,17] to the periodic setting, while relatively straightforward, is important for applications.
- Knowledge exchange: We show how the damped Newton method from the mathematical theory of semi-discrete optimal transport [14]

* Corresponding author.
E-mail address: d.bourne@hw.ac.uk (D.P. Bourne).

https://doi.org/10.1016/j.mechrescom.2022.104023
Received 27 July 2022; Received in revised form 3 November 2022; Accepted 22 November 2022
Available online 9 December 2022

can be used to generate RVEs of polycrystalline materials with grains of given volumes.

- Software: All our code is available on GitHub.
  MATLAB-Voro: MATLAB mex files for generating 2D and 3D periodic and non-periodic Laguerre tessellations using Voro++ [18]. https://github.com/smr29git/MATLAB-Voro
  MATLAB-SDOT: MATLAB functions for solving semi-discrete optimal transport problems using the damped Newton method. https://github.com/DPBourne/MATLAB-SDOT
  Laguerre-Polycrystalline-Microstructures: MATLAB functions for generating RVEs of polycrystalline microstructures using Laguerre tessellations, including all the examples from this paper. https://github.com/DPBourne/Laguerre-Polycrystalline-Microstructures

2. Periodic semi-discrete optimal transport

2.1. Notation

Throughout this paper $|x|$ denotes the standard Euclidean norm of a vector $x \in \mathbb{R}^d$.

Periodic domain. First we define a general class of periodic domains that includes the flat cylinder, flat torus and triply-periodic cuboid. Let $\Lambda \subset \mathbb{R}^d$, $d \geq 2$, be the integer span of $1 \leq k \leq d$ linearly independent vectors $v_1, \dots, v_k \in \mathbb{R}^d$, i.e.,

$$\Lambda = \text{span}_{\mathbb{Z}}\{v_1, \dots, v_k\}.$$

If $k = d$, then Λ is a *lattice*. Let

$$V = \{x \in \mathbb{R}^d : |x| \leq |x - u| \ \forall\, u \in \Lambda\}.$$

In other words, V is the fundamental *Voronoi cell* in the periodic Voronoi tessellation of $\mathbb{R}^d$ generated by Λ. For example, if $d = 2$, $k = 1$, $v_1 = (1, 0)$, then $V = [-1/2, 1/2] \times \mathbb{R}$ is the fundamental domain of the flat cylinder. If $d = 2$, $k = 2$, $v_1 = (1, 0)$, $v_2 = (0, 1)$, then $V = [-1/2, 1/2] \times [-1/2, 1/2]$ is the fundamental domain of the flat torus. For the microstructure application in Section 4, Λ and V are given in Eqs. (4.1) and (4.2).

Transport cost. Let $c_\Lambda : \mathbb{R}^d \times \mathbb{R}^d \to \mathbb{R}$ be the periodic quadratic transport cost defined by

$$c_\Lambda(x, y) = |x - y|_\Lambda^2 := \inf_{u \in \Lambda} |x - y - u|^2.$$

Observe that c_Λ is continuous but not differentiable, which is why the results of [14,15,17] do not immediately apply. For example, for the case of the flat torus given above with $d = 2$, $k = 2$, $v_1 = (1, 0)$, $v_2 = (0, 1)$, then $c_\Lambda((0, 0), (t, 0)) = \min\{t^2, (1 - t)^2\}$ for $t \in [0, 1]$, which is not differentiable as a function of t at $t = 1/2$. Note that the infimum in the definition of c_Λ is actually a minimum since $|x - y - u| \to \infty$ as $|u| \to \infty$.

Source measure. Let $\rho \in L^1(V; [0, \infty))$ and let $\mu = \rho\, \mathcal{L}^d \llcorner V$ be the measure on V that is absolutely continuous with respect to the Lebesgue measure with density ρ. For example, for the microstructure application we take $d = 3$, $\rho(x) = 1$ for all $x \in V$ so that $\mu(A)$ is the volume of a set $A \subseteq V$. In general, we assume that the support of μ is contained in a compact, convex subset X of V and that the restriction of ρ to X is Hölder continuous.

Extend ρ to $\mathbb{R}^d$ by Λ-periodicity, namely, define $\rho_\Lambda : \mathbb{R}^d \to [0, \infty)$ by $\rho_\Lambda(x + u) = \rho(x)$ for all $x \in V$, $u \in \Lambda$ (this defines ρ_Λ uniquely a.e.). Define $\mu_\Lambda = \rho_\Lambda\, \mathcal{L}^d$. Then μ_Λ satisfies $\mu_\Lambda \llcorner V = \mu$ and

$$\mu_\Lambda(A) = \mu_\Lambda(A + u) \tag{2.1}$$

for all $u \in \Lambda$ and Lebesgue-measurable sets $A \subset \mathbb{R}^d$.

Target measure. Let $Y \subset \text{int}(V)$ be a finite set. We call its elements *seeds*. Let $m : Y \to (0, \infty)$, $y \mapsto m_y$. Define the discrete measure $\nu := \sum_{y \in Y} m_y \delta_y$, where δ_y denotes the Dirac measure supported at y. We assume that $\sum_{y \in Y} m_y = \mu(V)$ so that $\nu(V) = \mu(V)$. Throughout this paper $n = \#Y$. For the microstructure application the m_y are the target volumes of the n grains.

Periodic laguerre tessellations. For each seed $y \in Y$, we associate a *weight* $w_y \in \mathbb{R}$. Let w be the *weight map* $w : Y \to \mathbb{R}$, $y \mapsto w_y$. For each $y \in Y$, we define the *periodic Laguerre cell*

$$L_y^\Lambda(w; Y) := \{x \in V : |x - y|_\Lambda^2 - w_y \leq |x - z|_\Lambda^2 - w_z \ \forall\, z \in Y\}.$$

The collection of all cells $\{L_y^\Lambda(w; Y)\}_{y \in Y}$ is the *periodic Laguerre tessellation of* V generated by (Y, w).

2.2. The optimal transport problem

The *Kantorovich function* $\mathcal{K}^\Lambda : \mathbb{R}^n \to \mathbb{R}$ is

$$\mathcal{K}^\Lambda(w) = \sum_{y \in Y} \int_{L_y^\Lambda(w;Y)} (|x - y|_\Lambda^2 - w_y)\, \mathrm{d}\mu(x) + \sum_{y \in Y} m_y w_y. \tag{2.2}$$

The (dual) periodic semi-discrete optimal transport problem is the optimisation problem

$$\max\left\{\mathcal{K}^\Lambda(w) : w \in \mathbb{R}^n\right\}.$$

The map $\mathcal{K}^\Lambda$ is concave and its critical points satisfy

$$\mu\big(L_y^\Lambda(w; Y)\big) = m_y$$

(see Theorem 2.5). Hence, if $w \in \text{argmax}\, \mathcal{K}^\Lambda$, then the periodic Laguerre tessellation $\{L_y^\Lambda(w; Y)\}_{y \in Y}$ has cells of masses $\{m_y\}_{y \in Y}$. For example, the cells have volumes $\{m_y\}_{y \in Y}$ if $\rho = 1$.

2.3. Regularity of the Kantorovich function

In this section we prove that $\mathcal{K}^\Lambda$ is twice continuously differentiable and compute its first and second derivatives. To overcome the lack of smoothness of c^Λ, we rewrite L_y^Λ and $\mathcal{K}^\Lambda$ in terms of the standard quadratic cost and standard Laguerre cells. Then the regularity of $\mathcal{K}^\Lambda$ follows easily from [14,15].

Definition 2.1. Given $y_1, y_2 \in \mathbb{R}^d$, we write $y_1 \sim y_2$ if $y_1 - y_2 \in \Lambda$. We say that $\overline{y} \in \mathbb{R}^d$ is a periodic copy of a seed $y \in Y$ if $\overline{y} \sim y$. Define $\overline{Y}$ to be the set of all periodic copies of the seeds in Y, namely

$$\overline{Y} = Y + \Lambda = \{y + u : y \in Y,\ u \in \Lambda\}.$$

If $\overline{y} \in \overline{Y}$, $\overline{y} \sim y \in Y$, we assign $\overline{y}$ the weight $w_{\overline{y}} := w_y$. Note that if $y_1 \sim y_2$, then $w_{y_1} = w_{y_2}$. Define the extended weight map $\overline{w} : \overline{Y} \to \mathbb{R}$, $\overline{y} \mapsto w_{\overline{y}}$. Given a domain $\Omega \subseteq \mathbb{R}^d$, the non-periodic Laguerre tessellation $\{L_{\overline{y}}(\overline{w}; \Omega, \overline{Y})\}_{\overline{y} \in \overline{Y}}$ of Ω generated by the extended set of seeds and weights $(\overline{Y}, \overline{w})$ is given by

$$L_{\overline{y}}(\overline{w}; \Omega, \overline{Y}) := \{x \in \Omega : |x - \overline{y}|^2 - \overline{w}_{\overline{y}} \leq |x - z|^2 - \overline{w}_z \ \forall\, z \in \overline{Y}\}.$$

Lemma 2.1. *The periodic Laguerre cells can be written in terms of the non-periodic cells as*

$$L_y^\Lambda(w; Y) = \bigcup_{u \in \Lambda} L_{y+u}(\overline{w}; V, \overline{Y}). \tag{2.3}$$

Proof. Let $x \in L_y^\Lambda(w; Y)$. By definition we have

$$|x - y|_\Lambda^2 - w_y \leq |x - z|_\Lambda^2 - w_z \quad \forall\, z \in Y.$$

Hence there exists $u_{xy} \in \Lambda$ such that, for all $z \in Y$,

$$\begin{aligned} |x - y - u_{xy}|^2 - w_y &\leq |x - z|_\Lambda^2 - w_z \\ &\leq |x - z - u|^2 - w_z \quad \forall\, u \in \Lambda. \end{aligned}$$

Observe that $\overline{w}_{y+u_{xy}} = w_y$ and $\overline{w}_{z+u} = w_z$. Therefore the previous inequality can be restated as

$$|x-(y+u_{xy})|^2 - \overline{w}_{y+u_{xy}} \le |x-\overline{z}|^2 - \overline{w}_{\overline{z}} \quad \forall\, \overline{z} \in \overline{Y}.$$

Therefore $x \in L_{y+u_{xy}}(\overline{w}; V, \overline{Y})$ and so

$$L_y^{\Lambda}(w;Y) \subseteq \bigcup_{u\in\Lambda} L_{y+u}(\overline{w}; V, \overline{Y}).$$

Now we prove the reverse inclusion. Let $x \in L_{y+u}(\overline{w}; V, \overline{Y})$ for some $u \in \Lambda$. By definition,

$$\begin{aligned}|x-y|_\Lambda^2 - w_y &\le |x-y-u|^2 - \overline{w}_{y+u}\\ &\le |x-\overline{z}|^2 - \overline{w}_{\overline{z}} \quad \forall\, \overline{z} \in \overline{Y}\end{aligned}$$

where the second inequality follows from the fact that $x \in L_{y+u}(\overline{w}; V, \overline{Y})$. Therefore

$$|x-y|_\Lambda^2 - w_y \le |x-z-u|^2 - w_z \quad \forall\, z \in Y,\ u \in \Lambda.$$

Taking the minimum over u gives

$$|x-y|_\Lambda^2 - w_y \le |x-z|_\Lambda^2 - w_z \quad \forall\, z \in Y.$$

Therefore $x \in L_y^{\Lambda}(w;Y)$, as required. □

Lemma 2.2. *The μ-measure of the periodic Laguerre cells can be expressed in terms of the measure of the non-periodic Laguerre cells as follows:*

$$\mu(L_y^{\Lambda}(w;Y)) = \sum_{u\in\Lambda} \mu\left(L_{y+u}(\overline{w}; V, \overline{Y})\right) = \mu_\Lambda(L_y(\overline{w}; \mathbb{R}^d, \overline{Y})).$$

Proof. The first equality follows immediately from Lemma 2.1 and the fact that the Laguerre cells $\{L_{y+u}(\overline{w}; V, \overline{Y})\}_{u\in\Lambda}$ are disjoint up to a set of measure zero since μ is absolutely continuous. Now we turn our attention to the second equality. Let $y \in Y$. We claim that

$$L_y(\overline{w}; \mathbb{R}^d, \overline{Y}) = \bigcup_{u\in\Lambda} \left(L_{y+u}(\overline{w}; V, \overline{Y}) - u\right). \tag{2.4}$$

Let $x \in L_y(\overline{w}; \mathbb{R}^d, \overline{Y})$. Then

$$|x-y|^2 - \overline{w}_y \le |x-z|^2 - \overline{w}_z \quad \forall\, z \in \overline{Y}.$$

Choose $u \in \Lambda$ so that $x+u \in V$. Then we can rewrite the previous inequality as

$$|x+u-(y+u)|^2 - \overline{w}_{y+u} \le |x-z|^2 - \overline{w}_z \quad \forall\, z \in \overline{Y}.$$

Therefore $x+u \in L_{y+u}(\overline{w}; V, \overline{Y})$ and so

$$L_y(\overline{w}; \mathbb{R}^d, \overline{Y}) \subseteq \bigcup_{u\in\Lambda} \left(L_{y+u}(\overline{w}; V, \overline{Y}) - u\right).$$

Conversely, take $x \in L_{y+u}(\overline{w}; V, \overline{Y}) - u$ for some $u \in \Lambda$. For all $z \in \overline{Y}$,

$$|x-y|^2 - \overline{w}_y = |x+u-(y+u)|^2 - \overline{w}_y \le |x-z|^2 - \overline{w}_z.$$

Therefore $x \in L_y(\overline{w}; \mathbb{R}^d, \overline{Y})$ and (2.4) follows.

Next we prove that $\{L_{y+u}(\overline{w}; V, \overline{Y}) - u\}_{u\in\Lambda}$ are disjoint sets up to a set of measure zero. Suppose that $x \in L_{y+u_i}(\overline{w}; V, \overline{Y}) - u_i$ for $i \in \{1,2\}$, $u_1, u_2 \in \Lambda$, $u_1 \ne u_2$. Then $x+u_i \in V$. By definition of V,

$$|x+u_i| \le |x+u_i-u| \quad \forall\, u \in \Lambda$$

for $i \in \{1,2\}$. That is,

$$|x-(-u_i)| \le |x-u| \quad \forall\, u \in \Lambda.$$

In other words, x lies in the Voronoi cells with generators $-u_1$ and $-u_2$ in the Voronoi tessellation of $\mathbb{R}^d$ generated by Λ. But the intersection of Voronoi cells is a set of measure zero, as desired.

Combining everything and using $\mu_\Lambda \llcorner V = \mu$ gives

$$\sum_{u\in\Lambda} \mu\left(L_{y+u}(\overline{w}; V, \overline{Y})\right) \overset{(2.1)}{=} \sum_{u\in\Lambda} \mu_\Lambda\left(L_{y+u}(\overline{w}; V, \overline{Y}) - u\right)$$
$$\overset{(2.4)}{=} \mu_\Lambda\left(L_y(\overline{w}; \mathbb{R}^d, \overline{Y})\right)$$

as required. □

Lemma 2.3. *$\mathcal{K}^{\Lambda}$ can be written in terms of the non-periodic transport cost and Laguerre cells as*

$$\mathcal{K}^{\Lambda}(w) - \sum_{y\in Y} m_y w_y = \sum_{y\in Y} \int_{L_y(\overline{w};\mathbb{R}^d,\overline{Y})} \left(|x-y|^2 - w_y\right) \mathrm{d}\mu_\Lambda(x) \tag{2.5}$$

$$= \sum_{y\in\overline{Y}} \int_{L_y(\overline{w};V,\overline{Y})} \left(|x-y|^2 - \overline{w}_y\right) \mathrm{d}\mu(x). \tag{2.6}$$

Proof. Let $y \in Y$, $u \in \Lambda$, $x \in L_{y+u}(\overline{w}; V, \overline{Y})$. We claim that

$$|x-y|_\Lambda = |x-y-u|. \tag{2.7}$$

To prove this observe that

$$\begin{aligned}|x-y-u|^2 &= |x-(y+u)|^2 - \overline{w}_{y+u} + \overline{w}_{y+u}\\ &\le |x-(y+v)|^2 \underbrace{-\overline{w}_{y+v} + \overline{w}_{y+u}}_{=0}\end{aligned}$$

for all $v \in \Lambda$. Therefore

$$|x-y-u| = \min_{v\in\Lambda} |x-y-v| = |x-y|_\Lambda$$

as claimed. For all $y \in Y$,

$$\begin{aligned}&\int_{L_y^{\Lambda}(w;Y)} (|x-y|_\Lambda^2 - w_y)\,\mathrm{d}\mu(x)\\ &\overset{(2.3)}{=} \int_{\bigcup_{u\in\Lambda} L_{y+u}(\overline{w};V,\overline{Y})} (|x-y|_\Lambda^2 - w_y)\,\mathrm{d}\mu(x)\\ &\overset{(2.7)}{=} \int_{\bigcup_{u\in\Lambda} L_{y+u}(\overline{w};V,\overline{Y})} (|x-y-u|^2 - w_y)\,\mathrm{d}\mu(x)\\ &= \sum_{u\in\Lambda} \int_{L_{y+u}(\overline{w};V,\overline{Y})} (|x-(y+u)|^2 - w_y)\,\mathrm{d}\mu(x).\end{aligned} \tag{2.8}$$

Combining this with the definition of $\mathcal{K}^{\Lambda}(w)$ gives

$$\begin{aligned}\mathcal{K}^{\Lambda}(w) - \sum_{y\in Y} m_y w_y &= \sum_{y\in Y}\sum_{u\in\Lambda} \int_{L_{y+u}(\overline{w};V,\overline{Y})} (|x-(y+u)|^2 - w_y)\,\mathrm{d}\mu(x)\\ &= \sum_{\overline{y}\in\overline{Y}} \int_{L_{\overline{y}}(\overline{w};V,\overline{Y})} (|x-\overline{y}|^2 - \overline{w}_{\overline{y}})\,\mathrm{d}\mu(x).\end{aligned}$$

This proves (2.6).

Using the substitution $x' = x-u$ in (2.8) gives

$$\begin{aligned}&\int_{L_y^{\Lambda}(w;Y)} (|x-y|_\Lambda^2 - w_y)\,\mathrm{d}\mu(x)\\ &= \int_{\bigcup_{u\in\Lambda}(L_{y+u}(\overline{w};V,\overline{Y})-u)} (|x'-y|^2 - w_y)\,\mathrm{d}\mu_\Lambda(x')\\ &= \int_{L_y(\overline{w};\mathbb{R}^d,\overline{Y})} (|x'-y|^2 - w_y)\,\mathrm{d}\mu_\Lambda(x')\end{aligned}$$

by (2.4). This proves (2.5), as required. □

In Theorems 2.4 and 2.5 we enumerate the seeds $y_1, \dots, y_M$ for some $M \in \mathbb{N}$, and in an abuse of notation we let w denote both the weight map $w : y_i \mapsto w_{y_i} \in \mathbb{R}$ and the vector $(w_1, \dots, w_M) := (w_{y_1}, \dots, w_{y_M})$.

First we recall a result from [14] (Theorems 1.3 & 4.1) about the regularity of the Kantorovich function for the standard (non-periodic) quadratic cost (see also [17, Proposition 2], [15, Theorem 45]).

Theorem 2.4 (*[14]*). *Let $Y = \{y_1, \dots, y_N\} \subset V$ be a set of distinct seeds. Define $g : \mathbb{R}^N \to \mathbb{R}$ by*

$$g(w) = \sum_{y\in Y} \int_{L_y(w;V,Y)} (|x-y|^2 - w_y)\,\mathrm{d}\mu(x).$$

Then $g \in C^1(\mathbb{R}^N)$ is concave with

$$\frac{\partial g}{\partial w_i}(w) = -\mu\big(L_{y_i}(w;V,Y)\big), \quad i \in \{1, \dots, N\}.$$

For $i, j \in \{1, \dots, N\}$, define

$$L_{y_i y_j}(w; V, Y) = L_{y_i}(w; V, Y) \cap L_{y_j}(w; V, Y)$$

(this may be the empty set). On the set

$$\left\{ w \in \mathbb{R}^N \,:\, \mu\big(L_y(w; V, Y)\big) > 0 \;\forall\, y \in Y \right\} \tag{2.9}$$

g is twice continuously differentiable and, for $i \neq j$,

$$\frac{\partial^2 g}{\partial w_i \partial w_j}(w) = \int_{L_{y_i y_j}(w;V,Y)} \frac{\rho(x)}{2|y_i - y_j|}\, \mathrm{d}\mathcal{H}^{d-1}(x),$$

$$\frac{\partial^2 g}{\partial w_i^2}(w) = -\sum_{\substack{j=1 \\ j\neq i}}^{N} \frac{\partial^2 g}{\partial w_i \partial w_j}(w).$$

Here $\mathcal{H}^{d-1}$ denotes the $(d-1)$-dimensional Hausdorff measure. Now we extend Theorem 2.4 to the periodic cost.

Theorem 2.5. *Let $Y = \{y_1, \dots, y_n\} \subset \mathrm{int}(V)$ be a set of distinct seeds. The Kantorovich function $\mathcal{K}^\Lambda \in C^1(\mathbb{R}^n)$ is concave with*

$$\frac{\partial \mathcal{K}^\Lambda}{\partial w_i}(w) = m_{y_i} - \mu\big(L^\Lambda_{y_i}(w; Y)\big), \quad i \in \{1, \dots, n\}.$$

Fix $w \in \mathbb{R}^n$. Let

$$\tilde{Y} = \tilde{Y}(w) = \{ y \in \overline{Y} \,:\, L_y(\overline{w}; V, \overline{Y}) \neq \emptyset \}$$

and let $\tilde{w} = \overline{w}|_{\tilde{Y}}$ be the restriction of $\overline{w}$ to $\tilde{Y}$. If $Y \subset \tilde{Y}(w)$ and

$$\mu\big(L_y(\tilde{w}; V, \tilde{Y}(w))\big) > 0 \quad \forall\, y \in \tilde{Y}(w), \tag{2.10}$$

then $\mathcal{K}^\Lambda$ is twice continuously differentiable at w and, for $i \neq j$,

$$\frac{\partial^2 \mathcal{K}^\Lambda}{\partial w_i \partial w_j}(w) = \sum_{\substack{y, y' \in \overline{Y} \\ y \sim y_i \\ y' \sim y_j}} \int_{L_{yy'}(\overline{w};V,\overline{Y})} \frac{\rho(x)}{2|y - y'|}\, \mathrm{d}\mathcal{H}^{d-1}(x)$$

$$\frac{\partial^2 \mathcal{K}^\Lambda}{\partial w_i^2}(w) = -\sum_{\substack{j=1 \\ j\neq i}}^{n} \frac{\partial^2 \mathcal{K}^\Lambda}{\partial w_i \partial w_j}(w).$$

Proof. Step 1. We prove that $\tilde{Y}$ is a finite set.

Step 1a. First we show that the Voronoi cell V is bounded in the periodic directions. By definition of V, for all $x \in V$, $i \in \{1, \dots, k\}$,

$$|x \cdot v_i| \leq \frac{1}{2}|v_i|^2 \leq \frac{1}{2} \max_{j \in \{1,\dots,k\}} |v_j|^2 =: \frac{1}{2} M^2. \tag{2.11}$$

Step 1b. Next we show that the Laguerre cells are bounded in the periodic directions. Let $x \in L_y(\overline{w}; \mathbb{R}^d, \overline{Y})$, $y \in Y$. For all $i \in \{1, \dots, k\}$,

$$|x - y|^2 - w_y \leq |x - (y + v_i)|^2 - \overline{w}_{y+v_i}.$$

Since $\overline{w}_{y+v_i} = w_y$, we obtain the bound

$$x \cdot v_i \leq \frac{1}{2}|v_i|^2 + y \cdot v_i \leq \frac{1}{2} M^2 + M \max_{y \in Y} |y| \;:= C.$$

By replacing v_i with $-v_i$ we obtain

$$|x \cdot v_i| \leq C.$$

Step 1c. It is an easy exercise to check that

$$L_{y+u}(\overline{w}; \mathbb{R}^d, \overline{Y}) = L_y(\overline{w}; \mathbb{R}^d, \overline{Y}) + u \;\; \forall\, y \in Y,\, u \in \Lambda.$$

Step 1d. Finally, we show that $\tilde{Y}$ is finite. Take $u = \sum_{i=1}^k a_i v_i$ where $a = (a_1, \dots, a_k) \in \mathbb{Z}^k$. Assume that

$$|a| > \sqrt{k}\left(\frac{1}{2} M^2 + C\right) \|G^{-1}\|_2 =: c \tag{2.12}$$

where $G \in \mathbb{R}^{k \times k}$ is the Gram matrix with components $G_{ij} = v_i \cdot v_j$ and $\|\cdot\|_2$ is the matrix 2-norm. We will show that, for all $y \in Y$,

$$L_{y+u}(\overline{w}; V, \overline{Y}) = \emptyset,$$

which proves that $\tilde{Y}$ is finite. In particular,

$$\tilde{Y} \subseteq \left\{ y + u \,:\, y \in Y,\, u = \sum_{i=1}^k a_i v_i,\, a \in \mathbb{Z}^k,\, |a| \leq c \right\}.$$

Let $b \in \mathbb{R}^k$ be the vector with components $b_i = u \cdot v_i$. Then $a = G^{-1} b$ and

$$|a| \leq \|G^{-1}\|_2\, |b| \leq \sqrt{k}\, \|G^{-1}\|_2\, |b|_\infty. \tag{2.13}$$

Take $\overline{x} \in L_{y+u}(\overline{w}; \mathbb{R}^d, \overline{Y})$. Then $\overline{x} = x + u$ for some $x \in L_y(\overline{w}; \mathbb{R}^d, \overline{Y})$ by Step 1c. Take $i \in \{1, \dots, k\}$ with $|u \cdot v_i| = \max_{j \in \{1,\dots,k\}} |u \cdot v_j| = |b|_\infty$. Then

$$\begin{aligned} |\overline{x} \cdot v_i| &= |x \cdot v_i + u \cdot v_i| \\ &\geq |u \cdot v_i| - |x \cdot v_i| \\ &\geq \max_{j \in \{1,\dots,k\}} |u \cdot v_j| - C \\ &> \frac{1}{2} M^2 \end{aligned}$$

by Step 1b and (2.12), (2.13). But then $\overline{x} \notin V$ by Step 1a. Therefore $L_{y+u}(\overline{w}; V, \overline{Y}) = \emptyset$, as claimed.

Step 2. Next we prove that for all $y \in \tilde{Y}$,

$$L_y(\tilde{w}; V, \tilde{Y}) = L_y(\overline{w}; V, \overline{Y}). \tag{2.14}$$

If $x \in L_y(\overline{w}; V, \overline{Y})$, then

$$|x - y|^2 - \overline{w}_y \leq |x - z|^2 - \overline{w}_z$$

for all $z \in \overline{Y}$, hence for all $z \in \tilde{Y}$ since $\tilde{Y} \subseteq \overline{Y}$. Therefore $L_y(\overline{w}; V, \overline{Y}) \subseteq L_y(\tilde{w}; V, \tilde{Y})$. Now we prove the opposite inclusion. Let $x \in L_y(\tilde{w}; V, \tilde{Y})$. Suppose for contradiction that $x \notin L_y(\overline{w}; V, \overline{Y})$. Then $x \in L_z(\overline{w}; V, \overline{Y})$ for some $z \in \overline{Y}$, $z \neq y$. Moreover, $z \in \tilde{Y}$ else $L_z(\overline{w}; V, \overline{Y}) = \emptyset$. Therefore $x \in L_y(\tilde{w}; V, \tilde{Y}) \cap L_z(\tilde{w}; V, \tilde{Y})$ and so

$$|x - y|^2 - \tilde{w}_y = |x - z|^2 - \tilde{w}_z. \tag{2.15}$$

Since $x \notin L_y(\overline{w}; V, \overline{Y})$, there exists $u \in \overline{Y}$ such that

$$|x - y|^2 - \tilde{w}_y > |x - u|^2 - \overline{w}_u. \tag{2.16}$$

Since $x \in L_z(\overline{w}; V, \overline{Y})$,

$$|x - z|^2 - \tilde{w}_z \leq |x - v|^2 - \overline{w}_v \quad \forall\, v \in \overline{Y}. \tag{2.17}$$

Combining (2.15)–(2.17) gives

$$|x - z|^2 - \tilde{w}_z = |x - y|^2 - \tilde{w}_y > |x - u|^2 - \overline{w}_u \geq |x - z|^2 - \tilde{w}_z,$$

which is a contradiction. Hence $x \in L_y(\overline{w}; V, \overline{Y})$.

Step 3. Fix $w \in \mathbb{R}^n$. We prove that, under assumption (2.10), $\tilde{Y}(w)$ is independent of w in a neighbourhood of w.

Step 3a. Define $f : V \times \overline{Y} \to \mathbb{R}$ by

$$f(x, y) = |x - y|^2 - \overline{w}_y - \min_{z \in \tilde{Y}} (|x - z|^2 - \overline{w}_z).$$

Let $x \in V$, $y \in \overline{Y} \setminus \tilde{Y}$. Then, for some $u \in \tilde{Y}$, $u \neq y$, $x \in L_u(\tilde{w}; V, \tilde{Y}) = L_u(\overline{w}; V, \overline{Y})$ (by (2.14)) and so

$$f(x, y) = |x - y|^2 - \overline{w}_y - (|x - u|^2 - \overline{w}_u) > 0.$$

We can rewrite f as

$$f(x, y) = \max_{z \in \tilde{Y}} \left(2x \cdot (z - y) + |y|^2 - |z|^2 + \overline{w}_z - \overline{w}_y \right).$$

Hence $f(\cdot, y)$ is positive, convex and piecewise affine with finitely many slopes, and so $\inf_{x \in V} f(x, y) = \min_{x \in V} f(x, y) > 0$.

Step 3b. By Step 3a, we can define

$$\varepsilon = \frac{1}{2} \inf_{y \in \overline{Y} \setminus \tilde{Y}} \min_{x \in V} f(x, y).$$

In this step we show that $\varepsilon > 0$. Let $\phi : \overline{Y} \setminus \tilde{Y} \to \mathbb{R}$, $\phi(y) = \min_{x \in V} f(x, y) > 0$. Take any sequence $(y_n) \subset \overline{Y} \setminus \tilde{Y}$ with $|y_n| \to +\infty$. We

show that $\lim_{n\to\infty}\phi(y_n)=+\infty$, which implies that $2\varepsilon=\inf_{y\in\overline{Y}\setminus\tilde{Y}}\phi(y)=\min_{y\in\overline{Y}\setminus\tilde{Y}}\phi(y)>0$. Since Y is a finite set, there exists a subsequence (y_n) (not relabelled) such that $y_n=y+u_n$ with $y\in Y$, $u_n\in\Lambda$, $|u_n|\to+\infty$. Let $x_n\in\arg\min_{x\in V}f(x,y_n)$. If $u=\sum_{i=1}^k a_i v_i\in\Lambda$, then $a=G^{-1}b$ where G and b were defined in Step 1d. By (2.11),

$$\begin{aligned}|x_n\cdot u|&=\left|\sum_{i=1}^k a_i(v_i\cdot x_n)\right|\le\sqrt{k}\,\frac{1}{2}M^2|a|\\&\le\sqrt{k}\,\frac{1}{2}M^2\|G^{-1}\|_2|b|\\&\le k\,\frac{1}{2}M^3\|G^{-1}\|_2|u|=:K|u|.\end{aligned}$$

Since $Y\subset\tilde{Y}$,

$$\begin{aligned}\phi(y_n)&=f(x_n,y_n)\\&=\max_{z\in\tilde{Y}}\left(2x_n\cdot(z-y_n)+|y_n|^2-|z|^2+\overline{w}_z-\overline{w}_{y_n}\right)\\&\ge 2x_n\cdot(y-y_n)+|y_n|^2-|y|^2+\overline{w}_y-\overline{w}_{y_n}\\&=-2x_n\cdot u_n+|y+u_n|^2-|y|^2\\&\ge-2K|u_n|+|y+u_n|^2-|y|^2\to\infty\text{ as }n\to\infty,\end{aligned}$$

as required.

Step 3c. Let $\psi:Y\to\mathbb{R}$, $|(\psi_{y_1},\dots,\psi_{y_n})|<\varepsilon$, $x\in V$. Extend ψ to $\overline{Y}$ and $\tilde{Y}$ the usual way. Assume that $y\in\overline{Y}$, $y\notin\tilde{Y}(w)$. Then $x\in L_u(\tilde{w};V,\tilde{Y})$ for some $u\ne y$, $u\in\tilde{Y}$. Therefore

$$\begin{aligned}&|x-y|^2-(\overline{w}_y+\overline{\psi}_y)-[|x-u|^2-(\tilde{w}_u+\tilde{\psi}_u)]\\&=|x-y|^2-\overline{w}_y-\min_{z\in\tilde{Y}}[|x-z|^2-\tilde{w}_z]+\tilde{\psi}_u-\overline{\psi}_y\\&>|x-y|^2-\overline{w}_y-\min_{z\in\tilde{Y}}[|x-z|^2-\tilde{w}_z]-2\varepsilon\ge 0.\end{aligned}$$

Therefore $x\notin L_y(\overline{w}+\overline{\psi};V,\overline{Y})$. Since $x\in V$ was arbitrary, this implies that $L_y(\overline{w}+\overline{\psi};V,\overline{Y})=\emptyset$. Hence $y\notin\tilde{Y}(w+\psi)$, and $\overline{Y}\setminus\tilde{Y}(w)\subseteq\overline{Y}\setminus\tilde{Y}(w+\psi)$ for all $|\psi|<\varepsilon$.

To complete the proof of Step 3 we need to show that, under assumption (2.10), $\tilde{Y}(w)\subseteq\tilde{Y}(w+\psi)$ if ψ is sufficiently small. Let $y\in\tilde{Y}(w)$. The map $w\mapsto\mu(L_y(\overline{w};V,\overline{Y}))$ is continuous (cf. [15, Proposition 38(vii)]). Therefore there exists $\delta_y>0$ such that $\mu(L_y(\overline{w}+\overline{\psi};V,\overline{Y}))>0$ if $|\psi|<\delta_y$, which implies that $y\in\tilde{Y}(w+\psi)$. Take $\delta=\min_{y\in\tilde{Y}(w)}\delta_y>0$ since $\tilde{Y}(w)$ is finite. Therefore $\tilde{Y}(w)\subseteq\tilde{Y}(w+\psi)$ for all $|\psi|<\delta$, as required.

Step 4. Now we compute the gradient and Hessian of $\mathcal{K}^\Lambda$. Fix $w_0\in\mathbb{R}^n$. By (2.6) and (2.14), for w in a sufficiently small neighbourhood of w_0,

$$\mathcal{K}^\Lambda(w)=g(\tilde{w})+\sum_{y\in Y}m_y w_y,$$

where g is as in Theorem 2.4 with $N=|\tilde{Y}(w_0)|\ge n$ and with the set of seeds $\tilde{Y}(w_0)$ (which is fixed in the chosen neighbourhood of w_0).

Observe that $\mathcal{K}^\Lambda$ is concave since it is the sum of a linear function and the composition of the concave function g with the linear function $w\mapsto\tilde{w}$.

The gradient of $\mathcal{K}^\Lambda$ follows from the Chain Rule and Theorem 2.4:

$$\begin{aligned}\frac{\partial\mathcal{K}^\Lambda}{\partial w_y}(w_0)&=\sum_{z\in\tilde{Y}(w_0)}\frac{\partial g}{\partial\tilde{w}_z}(\tilde{w}_0)\frac{\partial\tilde{w}_z}{\partial w_y}(w_0)+m_y\\&=\sum_{\substack{z\in\tilde{Y}(w_0)\\ z\sim y}}\frac{\partial g}{\partial\tilde{w}_z}(\tilde{w}_0)+m_y\\&=-\sum_{\substack{z\in\tilde{Y}(w_0)\\ z\sim y}}\mu\big(L_z(\tilde{w}_0;V,\tilde{Y}(w_0))\big)+m_y\\&=-\mu(L_y^\Lambda(w_0;Y))+m_y\end{aligned}$$

by Lemma 2.2 and Eq. (2.14).

If assumption (2.10) holds for $w=w_0$, then $\tilde{w}_0$ belongs to the set (2.9) (with seeds $\tilde{Y}(w_0)$). Therefore $w\mapsto g(\tilde{w})$ is twice continuously differentiable at w_0 and so is $\mathcal{K}^\Lambda$. Let $y_i,y_j\in Y$, $i\ne j$. Applying the Chain Rule and Theorem 2.4 gives

$$\begin{aligned}\frac{\partial^2\mathcal{K}^\Lambda}{\partial w_i\partial w_j}(w_0)&=\sum_{\substack{z\in\tilde{Y}(w_0)\\ z\sim y_i}}\sum_{z'\in\tilde{Y}(w_0)}\frac{\partial^2 g}{\partial\tilde{w}_z\partial\tilde{w}_{z'}}(\tilde{w}_0)\frac{\partial\tilde{w}_{z'}}{\partial w_{y_j}}(w_0)\\&=\sum_{\substack{z\in\tilde{Y}(w_0)\\ z\sim y_i}}\sum_{\substack{z'\in\tilde{Y}(w_0)\\ z'\sim y_j}}\frac{\partial^2 g}{\partial\tilde{w}_z\partial\tilde{w}_{z'}}(\tilde{w}_0)\\&=\sum_{\substack{z,z'\in\tilde{Y}(w_0)\\ z\sim y_i,z'\sim y_j}}\int_{L_{zz'}(\tilde{w}_0;V,\tilde{Y}(w_0))}\frac{\rho(x)}{2|z-z'|}\,\mathrm{d}\mathcal{H}^{d-1}(x)\\&=\sum_{\substack{z,z'\in\overline{Y}\\ z\sim y_i,z'\sim y_j}}\int_{L_{zz'}(\overline{w}_0;V,\overline{Y})}\frac{\rho(x)}{2|z-z'|}\,\mathrm{d}\mathcal{H}^{d-1}(x)\end{aligned}$$

by Eq. (2.14). We also used the fact that $z\ne z'$ if $z\sim y_i$, $z'\sim y_j$, $y_i\ne y_j$, which follows from the assumption that $Y\subset\mathrm{int}(V)$.

Finally, the diagonal entries of the Hessian are obtained by differentiating the following expression with respect to w_i:

$$\sum_{j=1}^n\frac{\partial\mathcal{K}^\Lambda}{\partial w_j}(w_0)=\sum_{j=1}^n\left[m_{y_j}-\mu\big(L_{y_j}^\Lambda(w_0;Y)\big)\right]=0.$$

This concludes the proof. □

Remark 2.1. The Hessian of $\mathcal{K}^\Lambda$ can be rewritten as follows, which we found more convenient for computational purposes: For $i\ne j$,

$$\frac{\partial^2\mathcal{K}^\Lambda}{\partial w_i\partial w_j}(w)=\sum_{\substack{y\in\overline{Y}\\ y\sim y_j}}\int_{L_{y_i y}(\overline{w};\mathbb{R}^d,\overline{Y})}\frac{\rho_\Lambda(x)}{2|y_i-y|}\,\mathrm{d}\mathcal{H}^{d-1}(x).$$

3. The damped Newton method

Given $w\in\mathbb{R}^n$, let $H(w)\in\mathbb{R}^{n\times n}$ denote the Hessian matrix $D^2\mathcal{K}(w)$. If w satisfies (2.10), it can be shown that $H(w)$ is singular with 1-dimensional kernel spanned by $(1,1,\dots,1)\in\mathbb{R}^n$ ($H(w)$ is a weighted graph Laplacian matrix of a connected graph). Moreover, the $(n-1)\times(n-1)$ matrix $\hat{H}(w)$ obtained by deleting the last row and column of $H(w)$ is non-singular. Let $e(w)$ be the error

$$e(w)=\max_{y\in Y}\left|\frac{\partial\mathcal{K}^\Lambda}{\partial w_y}(w)\right|=\max_{y\in Y}\left\|\mu\big(L_y^\Lambda(w;Y)\big)-m_y\right\|.$$

We recall the damped Newton method of Kitagawa, Mérigot and Thibert [14] for maximising $\mathcal{K}^\Lambda$:

Initialisation. Choose $w^0\in\mathbb{R}^n$ such that

$$\mu\big(L_y^\Lambda(w^0;Y)\big)>0\quad\forall\,y\in Y,\tag{3.1}$$

i.e., all the Laguerre cells have positive mass. Let

$$\varepsilon:=\frac{1}{2}\min\left\{\min_{y\in Y}\mu\big(L_y^\Lambda(w^0;Y)\big),\min_{y\in Y}m_y\right\}>0.$$

Iteration step. Give w^{k-1}, define w^k as follows:

1. Define the Newton direction $d^k\in\mathbb{R}^{n-1}$ by solving the sparse symmetric positive definite linear system

   $$-\hat{H}(w^{k-1})\,d^k=b$$

   where $b_i=\partial\mathcal{K}^\Lambda/\partial w_i(w^{k-1})$, $i=1,\dots,n-1$.
2. Find the smallest value of $l_k\in\{0\}\cup\mathbb{N}$ such that $w^{k,l_k}\in\mathbb{R}^n$ defined by $w_n^{k,l_k}=0$,

   $$w_i^{k,l_k}=w_i^{k-1}+2^{-l_k}d_i^k,\ i\in\{1,\dots,n-1\},$$

   satisfies

   $$\min_{y\in Y}\mu\big(L_y^\Lambda(w^{k,l_k};Y)\big)\ge\varepsilon,$$

   $$e(w^{k,l_k})\le(1-2^{-(l_k+1)})\,e(w^{k-1}).$$
3. Define the Newton update $w^k:=w^{k,l_k}$.

Stopping condition. Terminate the algorithm when the mass percentage error is less than some prescribed tolerance $\eta \in [0, 100]$:

$$100 \cdot \max_{y \in Y} \frac{\left|\mu\big(L_y^{\Lambda}(w^k; Y)\big) - m_y\right|}{m_y} < \eta.$$

We refer to l_k as the number of *backtracking steps* at iteration k. If $l_k = 0$, then w^k is the standard Newton step for the nonlinear system $\nabla \mathcal{K}^{\Lambda}(w) = 0$. The backtracking ensures that the iterates w^k remain in the region where $\mathcal{K}^{\Lambda}$ is twice differentiable.

In [14] it is proved that, for a class of continuously differentiable transport costs c, the damped Newton method converges for any initial guess satisfying (3.1) with linear rate and asymptotic quadratic rate (see [14, Prop. 6.1]). While their result does not apply to our non-smooth cost c_{Λ}, we have observed quadratic convergence in numerical experiments and believe the proof can be easily extended.

4. RVEs of polycrystalline materials

We can apply the theory above to generate 3D polycrystalline microstructures. We take $d = 3$,

$$\Lambda = \operatorname{span}_{\mathbb{Z}}\{(L_1, 0, 0), (0, L_2, 0), (0, 0, L_3)\}, \tag{4.1}$$

$$V = \left[-\tfrac{L_1}{2}, \tfrac{L_1}{2}\right] \times \left[-\tfrac{L_2}{2}, \tfrac{L_2}{2}\right] \times \left[-\tfrac{L_3}{2}, \tfrac{L_3}{2}\right], \tag{4.2}$$

where $L_1, L_2, L_3 > 0$, and $\rho(x) = 1$ for all $x \in V$. Then $\mu(L_y^{\Lambda}(w; V))$ equals the volume of $L_y^{\Lambda}(w; V)$. For *any* choice of seeds y_i and any list of volumes m_i (such that $\sum_i m_i = L_1 L_2 L_3$), the damped Newton method generates grains with volumes m_i. The choice of the seeds y_i gives extra control over the RVE. Choosing the seeds at random can lead to very anisotropic grains. The following algorithm updates the seed locations iteratively in order to generate grains that are not too irregular (see below for a precise definition of 'regular'). It combines [2, Algorithm 2] with the damped Newton method.

Input. The number of grains n, the desired grain volumes $m_1, \dots, m_n$ with $\sum_i m_i = L_1 L_2 L_3$, the volume percentage error tolerance $\eta > 0$, and the number of regularisation (Lloyd) steps K.

Initialisation. Randomly select n distinct seeds $y_1^{(0)}, \dots, y_n^{(0)} \in \operatorname{int}(V)$. Set $Y_{(0)} := \{y_1^{(0)}, \dots, y_n^{(0)}\}$, $w_{(0)} := 0 \in \mathbb{R}^n$, and

$$L_i^{(0)} := L_{y_i^{(0)}}(\overline{w_{(0)}}; \mathbb{R}^d, \overline{Y_{(0)}}), \quad i \in \{1, \dots, n\}.$$

Iteration step. For $k = 1, \dots, K$:

1. *Regularisation.* Define $y_i^{(k)}$ to be the centroid

$$y_i^{(k)} = \frac{1}{\mu(L_i^{(k-1)})} \int_{L_i^{(k-1)}} x \, \mathrm{d}x.$$

Set $Y_{(k)} = \{y_1^{(k)}, \dots, y_n^{(k)}\}$.

2. *Damped Newton.* Apply the damped Newton method with initial guess $w^0 = 0 \in \mathbb{R}^n$ to find a weight vector $w_{(k)} \in \mathbb{R}^n$ satisfying

$$100 \cdot \max_i \frac{\left|\mu\Big(L^{\Lambda}_{y_i^{(k)}}(w_{(k)}; Y_{(k)})\Big) - m_i\right|}{m_i} < \eta.$$

For $i \in \{1, \dots, n\}$, define

$$L_i^{(k)} := L_{y_i^{(k)}}(\overline{w_{(k)}}; \mathbb{R}^d, \overline{Y_{(k)}}).$$

Output. Define $y_i := y_i^{(K)}$, $Y = \{y_1, \dots, y_n\}$, and $w = w_{(K)}$. Then the periodic Laguerre cells $L_{y_1}^{\Lambda}(w; V), \dots, L_{y_n}^{\Lambda}(w; V)$ have volumes $m_1, \dots, m_n$ up to η percentage error.

If K is large, then the outputted Laguerre tessellation is approximately a *centroidal Laguerre tessellation* [19]. This means that the seeds y_i are approximately the centroids of the grains, which results in grains that are more 'regular' (round).

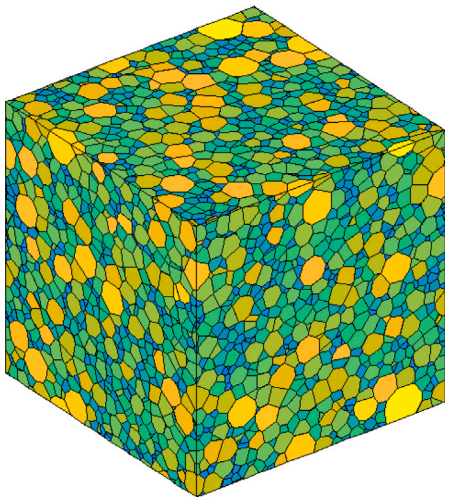

Fig. 1. A periodic Laguerre tessellation with 10,000 grains of prescribed volumes (up to 1% error), where the target volumes were drawn from a log-normal distribution; see Example 4.1. The grains are coloured according to their volume using a log scale. The large yellow polygons that are visible in the top face and the front-right face are slices through the same periodic grain. (For interpretation of the references to colour in this figure legend, the reader is referred to the web version of this article.)

The initial guess $w^0 = 0$ for the damped Newton steps satisfies assumption (3.1) since the corresponding Laguerre tessellation is a Voronoi tessellation, and Voronoi cells have positive volume when the seeds lie in the box.

The main difference between this algorithm and the one implemented in [2] is that we compute the weights using the 2nd-order damped Newton method instead of the slower 1st-order BFGS method. A rigorous study of various optimisation algorithms (steepest descent, Malitsky–Mishchenko, Barzilai–Borwein, BFGS, modified Newton) and regularisation steps (Lloyd, Anderson-accelerated Lloyd) is given in [3].

Example 4.1. We reproduce Example 5.5 from [2]. We take $n = 10{,}000$ grains, $L_1 = L_2 = L_3 = 2$, $K = 5$, $\eta = 1$. The target grain volumes m_i are drawn from a log-normal distribution as follows: First radii r_i are drawn from a log-normal distribution with mean 1 and standard deviation 0.35. Then we define $m_i = \frac{4}{3}\pi r_i^3$. Finally, the volumes are normalised so that the total volume of the grains equals the volume of the box. This is described further in [2, Example 5.5]. The RVE is shown in Fig. 1. This example took 47.24 s on a laptop with processor Intel(R) Core(TM) i5-1135G7 @ 2.40 GHz (cf. the run time of 669 s in [2, Example 5.5]).

5. Numerical tests of damped Newton

In this section we illustrate the performance of the damped Newton method from Section 3. In both examples Λ and V are given by (4.1), (4.2) with $L_1 = L_2 = L_3 = 1$ and $\rho(x) = 1$ for all $x \in V$ so that the damped Newton method generates Laguerre cells of given volumes.

Example 5.1. Table 1 reports mean run times of the damped Newton method over 100 numerical experiments for three types of microstructure.

The 1st column is the number of grains. The 2nd column is the mean run time for an idealised single phase (SP) microstructure, where all the grains have the same volume $m_i = L_1 L_2 L_3 / n$ for all i. The 3rd column is the mean run time for an idealised dual phase (DP) microstructure, where half of the grains have volume x and the other half have volume $5x$, where x is such that $\sum_i m_i = L_1 L_2 L_3$. The 4th column (log-normal) is the mean run time for a more realistic microstructure where the grain volumes are drawn from a log-normal distribution as in Example 4.1.

Table 1
Run times of the damped Newton method for generating Laguerre tessellations with n grains of given volumes (see Example 5.1), where all the grains have the same volume (SP), there are two grain sizes (DP), or the volumes are drawn from a log-normal distribution (log-normal).

n	Mean run time (s)		
	SP	DP	log-normal
100	0.03	0.09	0.06
250	0.07	0.16	0.23
500	0.18	0.34	0.53
1000	0.48	0.69	1.29
2500	1.30	1.82	3.51
5000	2.83	4.29	7.97
10,000	6.68	9.11	18.15
25,000	22.22	29.26	57.84
50,000	57.60	72.53	224.63
100,000	171.65	222.42	396.26

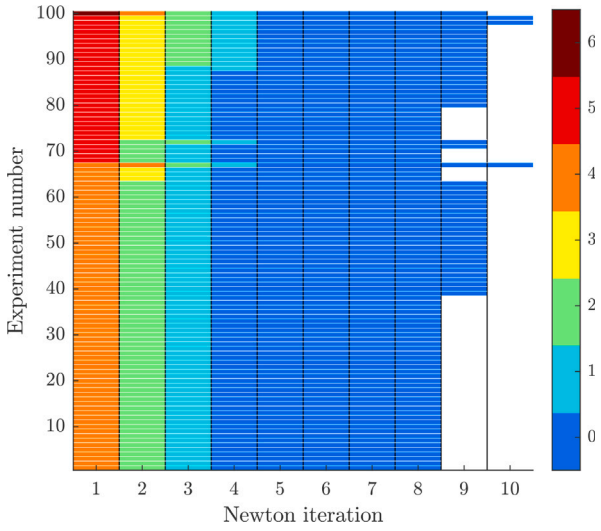

Fig. 2. The colour bar shows the number of backtracking steps for each Newton iteration, for each of 100 random log-normal microstructures with 100,000 grains (see Example 5.2). Each row in the figure is a single draw, the number of coloured blocks indicates the number of Newton iterations until the error tolerance is reached, and the colour of each block indicates the number of backtracking steps per Newton iteration. The draws have been sorted by the number of backtracking steps in each Newton iteration. (For interpretation of the references to colour in this figure legend, the reader is referred to the web version of this article.)

In all three experiments the seeds $y_1, \dots, y_n$ were drawn randomly from a uniform distribution and we average the run times over 100 draws. The volume tolerance is $\eta = 1\%$. We used the same laptop that was used for Example 4.1.

The run times grow superlinearly with respect to n but subquadratically. They increase as the complexity of the microstructure increases.

Example 5.2. Fig. 2 shows the number of Newton iterations and the number of backtracking steps l_k per Newton iteration for 100 random log-normal microstructures with $n = 100,000$ grains (as in the previous example). There is no backtracking at all after the 4th Newton iteration in any of the 100 experiments. In most experiments there is only one backtracking step in the 3rd Newton iteration. We do not observe the extensive backtracking in the early iterations reported in [3, Section 3.4].

6. Extensions

In principle the methods from this paper generalise to more exotic Laguerre diagrams. For example, non-periodic *generalised balanced power diagrams* (GBPDs) [1] with cells of given volumes can be found by maximising

$$\mathcal{K}_{\mathrm{GBPD}}(w) = \sum_{i=1}^{n} \int_{L_i(w;Y,A)} (|x - y_i|^2_{A_i} - w_i)\,\mathrm{d}x + \sum_{i=1}^{n} m_i w_i$$

where $A = \{A_1, \dots, A_n\}$ is a collection of symmetric positive definite matrices, $|\cdot|_{A_i}$ is the A_i-norm, given by $|x|^2_{A_i} = x \cdot A_i x$, and

$$L_i(w; Y, A) = \{x \in V : |x - y_i|^2_{A_i} - w_i \le |x - y_j|^2_{A_j} - w_j \ \forall\, j\}.$$

If $w \in \operatorname{argmax} \mathcal{K}_{\mathrm{GBPD}}$, then the cells $L_i(w; Y, A)$ have volumes m_i. Periodic GBPDs can be generated in a similar way. In practice it is challenging to compute GBPDs efficiently if there are many grains. We are currently working on this.

Declaration of competing interest

The authors declare that they have no known competing financial interests or personal relationships that could have appeared to influence the work reported in this paper.

Data availability

No data was used for the research described in the article.

Acknowledgements

The authors thank Piet Kok, Wil Spanjer, Carola Celada-Casero and Karo Sedighiani for fruitful discussions. DPB acknowledges financial support from the EPSRC, UK grant EP/V00204X/1. MP thanks the Centre for Doctoral Training in Mathematical Modelling, Analysis and Computation funded by EPSRC, UK grant EP/S023291/1.

References

[1] A. Alpers, A. Brieden, P. Gritzmann, A. Lyckegaard, H.F. Poulsen, Generalized balanced power diagrams for 3D representations of polycrystals, Phil. Mag. 95 (9) (2015) 1016–1028.
[2] D.P. Bourne, P.J.J. Kok, S.M. Roper, W.D.T. Spanjer, Laguerre tessellations and polycrystalline microstructures: A fast algorithm for generating grains of given volumes, Phil. Mag. 100 (21) (2020) 2677–2707.
[3] J. Kuhn, M. Schneider, P. Sonnweber-Ribic, T. Böhlke, Fast methods for computing centroidal Laguerre tessellations for prescribed volume fractions with applications to microstructure generation of polycrystalline materials, Comput. Methods Appl. Mech. Engrg. 369 (2020) 113175.
[4] I. Pérez, M. Muniz de Farias, M. Castro, R. Roselló, C. Recarey Morfa, L. Medina, E. Oñate, Modeling polycrystalline materials with elongated grains, Int. J. Numer. Methods. Eng. 118 (3) (2019) 121–131.
[5] R. Quey, L. Renversade, Optimal polyhedral description of 3D polycrystals: Method and application to statistical and synchrotron X-ray diffraction data, Comput. Methods Appl. Mech. Eng. 330 (2018) 308–333.
[6] K. Teferra, D.J. Rowenhorst, Direct parameter estimation for generalised balanced power diagrams, Philos. Mag. Lett. 98 (2) (2018) 79–87.
[7] T.F.W. van Nuland, J.A.W. van Dommelen, M.G.D. Geers, An anisotropic Voronoi algorithm for generating polycrystalline microstructures with preferred growth directions, Comput. Mater. Sci. 186 (2021) 109947.
[8] R. Chandrasekaran, M. Hillgärtner, A. Rege, B. Milow, M. Itskov, Geometric and finite element modeling of biopolymer aerogels to characterize their microstructural and mechanical properties, PAMM 21 (1) (2021) e202100122.
[9] F. Gehrig, D. Wicht, M. Krause, T. Böhlke, FFT-based investigation of the shear stress distribution in face-centered cubic polycrystals, Int. J. Plast. 157 (2022) 103369.
[10] L. Petrich, O. Furat, M. Wang, C.E. Krill, V. Schmidt, Efficient fitting of 3D tessellations to curved polycrystalline grain boundaries, Front. Mater. 8 (2021) 760602.
[11] L. Petrich, J. Staněk, M. Wang, D. Westhoff, L. Heller, P. Šittner, C.E. Krill, V. Beneš, V. Schmidt, Reconstruction of grains in polycrystalline materials from incomplete data using laguerre tessellations, Microsc. Microanal. 25 (3) (2019) 743–752.
[12] A. Alpers, M. Fiedler, P. Gritzmann, F. Klemm, Dynamic grain models via fast heuristics for diagram representations, 2022, arXiv:2204.06430.
[13] F. Santambrogio, Optimal Transport for Applied Mathematicians, Springer, 2015.
[14] J. Kitagawa, Q. Mérigot, B. Thibert, Convergence of a Newton algorithm for semi-discrete optimal transport, J. Eur. Math. Soc. 21 (9) (2019) 2603–2651.

[15] Q. Mérigot, B. Thibert, Optimal transport: discretization and algorithms, in: A. Bonito, R.H. Nochetto (Eds.), Handbook of Numerical Analysis: Geometric Partial Differential Equations - Part II, 22, 2021, pp. 133–212.
[16] C.P. Egan, D.P. Bourne, C.J. Cotter, M.J.P. Cullen, B. Pelloni, S.M. Roper, M. Wilkinson, A new implementation of the geometric method for solving the Eady slice equations, J. Comput. Phys. 469 (2022) 111542.
[17] F. de Gournay, J. Kahn, L. Lebrat, Differentiation and regularity of semi-discrete optimal transport with respect to the parameters of the discrete measure, Numer. Math. 141 (2) (2019) 429–453.
[18] C.H. Rycroft, Voro++: A three-dimensional Voronoi cell library in C++, Chaos 19 (2009) 041111.
[19] D.P. Bourne, S.M. Roper, Centroidal power diagrams, Lloyd's algorithm, and applications to optimal location problems, SIAM J. Numer. Anal. 53 (6) (2015) 2545–2569.